 FDMP, vol.11, no.1, pp.1-26, 2015

Theoretical Study of Solvation Effect on Diffusion Coefficient of Li Ion in Propylene Carbonate

Kentaro Doi[1,2], **Yuzuru Chikasako**[1] **and Satoyuki Kawano**[1,3]

Abstract: Propylene carbonate (PC) and ethylene carbonate are known as good candidates of organic solvents to be used in Li-ion rechargeable batteries, since Li^+ ions exhibit preferable charge-discharge characteristics with such solvents. On the other hand, polar solvents usually form solvation shells with solute ions, and cause a drastic reduction of ionic conductivity. Along these lines, there has been a curious question why the diffusion coefficient D_{Li} of Li^+ strongly depends on the salt concentration. In the present study, a theoretical model is developed on the basis of the Langevin equation in which the interactions between ions and solvent molecules are explicitly taken into account. Interesting phenomena, which were found in experiments but had not yet been theoretically clarified, are discussed in detail. Molecular dynamics (MD) simulations are also performed to elucidate the relationship between the solvation shell of Li^+ and D_{Li}. Analyzing the radial distribution function of PC molecules around Li^+ ions, the existence of first and second solvation shells (consisting of locally and highly concentrated PC molecules) is numerically clarified. In particular, overlapped regions of the second solvation shells are clearly observed, with the shell volume apparently increasing with an increase in the concentration of Li^+. This result indicates that the solvation structures can attractively interact with each other via overlaps of the second shells. The theoretical model and MD simulations are in excellent agreement with experimental data.

Keywords: Li-ion battery, Langevin equation, Molecular dynamics simulation, Diffusion coefficient, Solvation shell.

[1] Department of Mechanical Science and Bioengineering, Graduate School of Engineering Science, Osaka University, Toyonaka, Osaka 560–8531, Japan.
[2] E-mail: doi@me.es.osaka-u.ac.jp
[3] E-mail: kawano@me.es.osaka-u.ac.jp

1 Introduction

Lithium ion rechargeable batteries are known as a preferable power source for various electric devices, such as cell-phones, laptops, electric vehicles, and medical devices. Further improvements have been expected to supply more long-life operations and higher power densities, which result in downsizing and high performances of the batteries. Several review papers about this topic were published [Tarascon and Armad (2001); Aricò, Bruce, Scrosati, Tarascon, and Schalkwijk (2005); Zhang (2006)]. In recent experimental researches, the conductivity and diffusion coefficient of Li^+ were investigated as a function of the lithium salt concentration [Klassen, Aroca, Nazri, and Nazri (1998); Saito, Yamamoto, Nakamura, Kageyama, Ishikawa, Miyoshi, and Matsuoka (1999); Kondo, Sano, Hiwara, Omi, Fujita, Kuwae, Iida, Mogi, and Yokoyama (2000); Aihara, Arai, and Hayamizu (2000); Tsunekawa, Narumi, Sano, Hiwara, Fujita, and Yokoyama (2003); Zhao, Wang, He, Wan, and Jiang (2008); Takeuchi, Kameda, Umebayashi, Ogawa, Sonoda, Ishiguro, Fujita, and Sano (2009)]. Theoretical models predicted the electric properties of Li-ion rechargeable batteries [Newman, Thomas, Hafezi, and Wheeler (2003); Kawano and Nishimura (2005a); Kawano and Nishimura (2005b); Barbero, Evangelista, and Lelidis (2006); Barbero and Lelidis (2007); Kawano and Nishimura (2008)]. Computational studies based on conventional models [Newman, Thomas, Hafezi, and Wheeler (2003); Barbero, Evangelista, and Lelidis (2006); Barbero and Lelidis (2007); Lee and Rasaiah (1994); Soetens, Millot, and Maigret (1998); Li and Balbuena (1999); Arora, Doyle, Gozdz, White, and Newman (2000); Costa and Ribeiro (2007); Hamad, Novotny, Wipf, and Rikvold (2010)] and multiphase flow models [Kawano and Nishimura (2005a); Kawano and Nishimura (2005b); Kawano and Nishimura (2008)] were effective tools to simulate the charge and discharge characteristics. As a result, it was predicted that solvation structures around Li^+ ions and cation–anion pairs caused to reduce the battery performance.

In Li-ion batteries, electrolyte solutions usually consist of mixtures of polar organic solvents, e.g., propylene carbonate (PC), ethylene carbonate, dimethyl ether and dimethyl carbonate, which are known to improve the charge and discharge efficiencies. On the other hand, the solvation structures due to interactions between a Li^+ ion and surrounding solvent molecules are suspected to decrease the electrophoretic mobility of Li^+ [Klassen, Aroca, Nazri, and Nazri (1998); Saito, Yamamoto, Nakamura, Kageyama, Ishikawa, Miyoshi, and Matsuoka (1999); Kondo, Sano, Hiwara, Omi, Fujita, Kuwae, Iida, Mogi, and Yokoyama (2000); Aihara, Arai, and Hayamizu (2000); Tsunekawa, Narumi, Sano, Hiwara, Fujita, and Yokoyama (2003); Zhao, Wang, He, Wan, and Jiang (2008); Takeuchi, Kameda, Umebayashi, Ogawa, Sonoda, Ishiguro, Fujita, and Sano (2009)]. However, effects of

complexes of a Li^+ ion and solvent molecules on the power generation efficiency and rechargeability have not yet been elucidated. Herein, we tackle this problem by developing a theoretical model based on the Langevin equation, focusing on Li^+ ions that transport interacting with PC solvent molecules. Furthermore, by performing molecular dynamics (MD) simulations, sampling data are systematically analyzed in terms of the radial distribution function of PC molecules, diffusion coefficient D_{Li} of Li^+ ion, and molecular structures in the electrolyte solution.

It is found that some PC molecules, from 4 to 6 molecules, solvate to a Li^+ ion, where this structure is known as a solvation shell whose existence was predicted in previous studies [Saito, Yamamoto, Nakamura, Kageyama, Ishikawa, Miyoshi, and Matsuoka (1999); Kondo, Sano, Hiwara, Omi, Fujita, Kuwae, Iida, Mogi, and Yokoyama (2000)]. Furthermore, the existence of the second solvation shell, which is a highly concentrated region of PC molecules outer the first shell, is discussed. Within the practical range of Li^+ concentration, it is confirmed that overlaps of the second solvation shells become larger with increasing Li^+ concentrations. It is also predicted that interactions between Li^+ ions via the second solvation shells modulate D_{Li}. This study concludes that the reduction of D_{Li} is caused not only by the well-known Stokes drag on the first solvation shell, but also by the effect of the second shell.

Furthermore, electrically charged molecules and ions are also expected to transport in aqueous solutions in the same manner as Li^+ in organic polar solvents. Findings in this study may be applicable for ion transport in aqueous solutions [Doi, Ueda, and Kawano (2011); Doi, Tsutsui, Ohshiro, Chien, Zwolak, Taniguchi, Kawai, Kawano, and Di Ventra (2014)], molecular transport phenomena in micro/nanofluidics [Nakano, Ohta, Yokoe, Doi, and Tachibana (2006); Doi, Nakano, Ohta, and Tachibana (2007); Doi, Onishi, and Kawano (2011); Doi, Onishi, and Kawano (2012); Yasui, Rahong, Motoyama, Yanagida, Wu, Kaji, Kanai, Doi, Nagashima, Tokeshi, Taniguchi, Kawano, Kawai, and Baba (2013)], and manipulation techniques of molecular structures on substrate surfaces [Doi, Yoshida, Nakano, Tachibana, Tabata, Kojima, and Okazaki (2005); Doi, Takeuchi, Nii, Akamatsu, Kakizaki, and Kawano (2013); Doi, Toyokita, Akamatsu, and Kawano (2014)].

2 Theoretical methods of solution

2.1 Langevin equation for suspensions

As shown in Fig. 1(a), solute particles in uniform solutions are affected by surrounding solvent molecules. In a theoretical model, collisions between a solute particle and solvent molecules are often represented by the random force in terms of thermal fluctuations, which is known as the Brownian dynamics. There are some

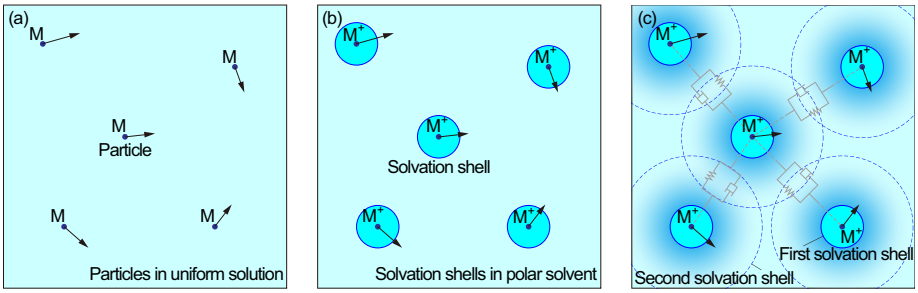

Figure 1: Schematic illustration of (a) isolated solute particles in uniform solution, (b) M^+ ions with solvation shells in polar solvents, which behave like a dilute suspension, and (c) densely solvated M^+ ions interacting with each other via the second solvation shells.

assumptions: a target particle is fully separated from solvents; collisions from the solvent molecules are isotropic; the motion of solute particles does not affect that of solvent molecules, that is, any historical effect is not considered. In such a case, the motion of a solute particle is effectively expressed by the Langevin equation [McQuarrie (2000)]:

$$m_i \frac{\mathrm{d}\mathbf{u}_i}{\mathrm{d}t} = -m_i \gamma_i \mathbf{u}_i + \mathbf{R}_i, \quad t \in (0, \infty), \tag{1}$$

where m_i is the mass of the ith species, $\mathbf{u}_i(t)$ the velocity, γ_i the collision frequency, and $\mathbf{R}_i(t)$ the random force due to the thermal fluctuations, which herein satisfies

$$\langle \mathbf{R}_i(t) \rangle = 0, \tag{2}$$

$$\langle \mathbf{R}_i(t) \cdot \mathbf{R}_j(t') \rangle = 6 k_\mathrm{B} T m_i \gamma_i \delta_{ij} \delta(t - t'), \tag{3}$$

where k_B is the Boltzmann constant, T temperature, δ_{ij} the Kronecker delta, and $\delta(t-t')$ the Dirac delta function. Solving Eq. 1 with the conditions of Eq. 2 and Eq. 3, we obtain

$$\mathbf{u}_i(t) = \mathbf{u}_{0i} \mathrm{e}^{-\gamma_i t} + \int_0^t \mathbf{R}_i \mathrm{e}^{-\gamma_i (t-t')} \mathrm{d}t', \tag{4}$$

and thus,

$$\langle \mathbf{u}_i \rangle = \mathbf{u}_{0i} \mathrm{e}^{-\gamma_i t}, \tag{5}$$

$$\left\langle |\mathbf{u}_i|^2 \right\rangle = \frac{3 k_\mathrm{B} T}{m_i} + \left(|\mathbf{u}_{0i}|^2 - \frac{3 k_\mathrm{B} T}{m_i} \right) \mathrm{e}^{-2\gamma_i t}, \tag{6}$$

where we set $\mathbf{u}_i(0) = \mathbf{u}_{0i}$. We focus on the behavior of ions in polar solvents, where ions form solvation shells as shown in Fig. 1(b) and collisions between them may affect the diffusivity. Furthermore, considering interactions between the solvation shells in dense suspensions as shown in Fig. 1(c), we suppose to modify Eq. 1 as

$$m_i \frac{\mathrm{d}\mathbf{u}_i}{\mathrm{d}t} = -m_i\gamma_i\mathbf{u}_i - \sum_{j\neq i}\xi_{ij}(\mathbf{u}_i - \mathbf{u}_j) - \sum_{j\neq i}\nabla\phi_{ij} + \mathbf{R}_i, \;\; t \in (0,\infty), \tag{7}$$

where ξ_{ij} has a role of the friction coefficient for energy dissipation resulting from the friction between the ith and jth solvation shells and ϕ_{ij} is a potential function for their interaction. The second and the third terms in the right-hand side in Eq. 7 describe that two particles are connected with both a spring and viscous damper in the suspension. When it is assumed that this long range interaction between solute ions is sufficiently weaker than thermal fluctuations and that Eq. 2 and Eq. 3 are maintained, solving Eq. 7, we obtain

$$\mathbf{u}_i(t) = \mathbf{u}_{0i}\mathrm{e}^{-\tilde{\gamma}_i t} + \frac{1}{m_i}\int_0^t (\mathbf{F}_i + \mathbf{R}_i)\,\mathrm{e}^{-\tilde{\gamma}_i(t-t')}\mathrm{d}t', \tag{8}$$

where

$$\mathbf{F}_i \equiv \sum_{j\neq i}\xi_{ij}\mathbf{u}_j - \sum_{j\neq i}\nabla\phi_{ij}, \tag{9}$$

$$\tilde{\gamma}_i \equiv \gamma_i\left(1 + \frac{1}{m_i\gamma_i}\sum_{j\neq i}\xi_{ij}\right). \tag{10}$$

Integrating Eq. 8, we obtain the displacement as

$$\mathbf{r}_i(t) - \mathbf{r}_i(0) = \frac{\mathbf{u}_{0i}}{\tilde{\gamma}_i}\left(1 - \mathrm{e}^{-\tilde{\gamma}_i t}\right) + \frac{1}{m_i\tilde{\gamma}_i}\int_0^t \left[1 - \mathrm{e}^{-\tilde{\gamma}_i(t-t')}\right](\mathbf{F}_i + \mathbf{R}_i)\,\mathrm{d}t'. \tag{11}$$

In this study, we discuss an equilibrium condition of suspensions in which solute particles are not driven by the externally applied force and thus,

$$\langle\mathbf{F}_i\rangle = \sum_{j\neq i}\xi_{ij}\langle\mathbf{u}_j\rangle - \left\langle\sum_{j\neq i}\nabla\phi_{ij}\right\rangle = 0. \tag{12}$$

At the limit of $t\to\infty$, $\langle\mathbf{u}_j\rangle = 0$ and then, $\left\langle\sum_{j\neq i}\nabla\phi_{ij}\right\rangle = 0$. This result means that the suspension is spatially isotropic. Furthermore, when it is assumed that $\sum_{j\neq i}\nabla\phi_{ij} \approx 0$ for the long-range weak interaction between the centers of solvation

shells, taking the ensemble average of the square displacement into account, we obtain

$$\begin{aligned}\left\langle \left|\mathbf{r}_i(t)-\mathbf{r}_i(0)\right|^2 \right\rangle &= \frac{\left|\mathbf{u}_{0i}\right|^2}{\tilde{\gamma}_i^2}\left(1-\mathrm{e}^{-\tilde{\gamma}_i t}\right)^2+\frac{3k_{\mathrm{B}}T\gamma_i}{m_i\tilde{\gamma}_i^3}\left(2\tilde{\gamma}_i t-3+4\mathrm{e}^{-\tilde{\gamma}_i t}-\mathrm{e}^{-2\tilde{\gamma}_i t}\right)\\ &+\frac{1}{m_i^2\tilde{\gamma}_i^2}\int_0^t\int_0^t\left[1-\mathrm{e}^{-\tilde{\gamma}_i(t-t')}-\mathrm{e}^{-\tilde{\gamma}_i(t-t'')}+\mathrm{e}^{-\tilde{\gamma}_i(2t-t'-t'')}\right]\\ &\times\left\langle \mathbf{F}_i(t')\cdot\mathbf{F}_i(t'')\right\rangle \mathrm{d}t'\mathrm{d}t''. \end{aligned} \tag{13}$$

Here, we adopted Eq. 2, Eq. 3 and Eq. 12. According to Eq. 9, at the limit of $t\to\infty$, we obtain

$$\left\langle \mathbf{F}_i(t')\cdot\mathbf{F}_i(t'')\right\rangle \approx \sum_{j\neq i}\xi_{ij}^2\left\langle \mathbf{u}_j(t')\cdot\mathbf{u}_j(t'')\right\rangle \tag{14}$$

In equilibrium, the superposition of the interacting force is considered to be nearly zero due to the uniform distribution of solute ions. For $\sum_{j\neq i}\xi_{ij}\ll m_i\gamma_i$, the last term on the right-hand side in Eq. 13 is reduced, since it is scaled by $\sum_{j\neq i}\xi_{ij}^2/(m_i\tilde{\gamma}_i)^2$ compared with the other terms. Therefore, Eq. 13 results in

$$\lim_{t\to\infty}\frac{1}{6t}\left\langle \left|\mathbf{r}_i(t)-\mathbf{r}_i(0)\right|^2\right\rangle = \frac{k_{\mathrm{B}}T\gamma_i}{m_i\tilde{\gamma}_i^2}=D_i^0\left(1+\frac{1}{m_i\gamma_i}\sum_{j\neq i}\xi_{ij}\right)^{-2}, \tag{15}$$

where

$$D_i^0=\frac{k_{\mathrm{B}}T}{m_i\gamma_i}=\frac{k_{\mathrm{B}}T}{6\pi\mu a_i} \tag{16}$$

is the diffusion coefficient in the free solution, μ is the viscosity of solvent, a_i is the hydrodynamic radius. Here, the Stokes–Einstein relation, $m_i\gamma_i=6\pi\mu a_i$, is employed between the middle and right-hand sides in Eq. 16. Effects of the suspension are namely represented by ξ_{ij}, which is evaluated by using MD simulations and previous experimental results. In the MD simulation, we investigate the solvation shells of Li^+ ions as a function of salt concentrations. The diffusion coefficient resulting from MD simulations is compared with Eq. 15.

2.2 Molecular dynamics simulation for Li^+ ions in PC solvent

It was reported that conductivity of Li^+ had a peak at 0.64×10^3 mol/m^3 [Tsunekawa, Narumi, Sano, Hiwara, Fujita, and Yokoyama (2003)] or 0.8×10^3 mol/m^3 [Kondo, Sano, Hiwara, Omi, Fujita, Kuwae, Iida, Mogi, and Yokoyama (2000)] and tended to rapidly decrease with increasing the number of Li^+ ions corresponding to the

lithium salt concentration ranging from 1.0×10^3 to 2.0×10^3 mol/m^3 [Klassen, Aroca, Nazri, and Nazri (1998); Kondo, Sano, Hiwara, Omi, Fujita, Kuwae, Iida, Mogi, and Yokoyama (2000); Tsunekawa, Narumi, Sano, Hiwara, Fujita, and Yokoyama (2003)]. However, the detailed mechanism of decrease in the conductivity has never been clarified yet. In this section, MD simulations are carried out to investigate the effect of solvation shells of Li^+ in PC solvent on the diffusivity. We assume that Li^+ ions are fully-ionized in PC solvent such as $LiA \rightarrow Li^+ + A^-$, where LiA and A^- represent a lithium salt and its anion, respectively. That is, the concentration c of Li^+ is equal to that of lithium salt in the previous experiments [Klassen, Aroca, Nazri, and Nazri (1998); Saito, Yamamoto, Nakamura, Kageyama, Ishikawa, Miyoshi, and Matsuoka (1999); Kondo, Sano, Hiwara, Omi, Fujita, Kuwae, Iida, Mogi, and Yokoyama (2000); Aihara, Arai, and Hayamizu (2000); Tsunekawa, Narumi, Sano, Hiwara, Fujita, and Yokoyama (2003); Zhao, Wang, He, Wan, and Jiang (2008); Takeuchi, Kameda, Umebayashi, Ogawa, Sonoda, Ishiguro, Fujita, and Sano (2009)]. Figure 2 shows schematic illustrations of Li^+ ions in PC solvent at $c = 1.08 \times 10^3$ mol/m^3. As shown in Fig. 2(a), it is clear that the number of Li^+ ions is much smaller than that of constituent atoms of PC and then, the effect of A^- on the behavior of Li^+ may be much smaller than that of PC molecules. Several numerical researches evaluated D_{Li}, taking the existence of anion into account [Takeuchi, Kameda, Umebayashi, Ogawa, Sonoda, Ishiguro, Fujita, and Sano (2009)]. However, the presence of anions near Li^+ often resulted in underestimate of D_{Li} in comparison with the experimental data [Saito, Yamamoto, Nakamura, Kageyama, Ishikawa, Miyoshi, and Matsuoka (1999); Aihara, Arai, and Hayamizu (2000); Tsunekawa, Narumi, Sano, Hiwara, Fujita, and Yokoyama (2003); Takeuchi, Kameda, Umebayashi, Ogawa, Sonoda, Ishiguro, Fujita, and Sano (2009)]. The experimental results imply that Li^+ and A^- are sufficiently separated in the solution in the range of $c < 2.0 \times 10^3$ mol/m^3 [Kondo, Sano, Hiwara, Omi, Fujita, Kuwae, Iida, Mogi, and Yokoyama (2000); Takeuchi, Kameda, Umebayashi, Ogawa, Sonoda, Ishiguro, Fujita, and Sano (2009)]. In previous studies, hydration structures were also investigated in highly polarized conditions, not only in organic solvents, but also in polar aqueous solutions [Lee and Rasaiah (1994); Koneshan, Rasaiah, Lynden-Bell, and Lee (1998)]. In the MD simulation, the number N_{Li} of Li^+ ions is set to a constant value of 50 in the computational cell. So, various c is realized by changing the cell volume Ω under the isothermal-isobaric condition. To compare the present simulations with the previous experiments, the number N_{PC} of PC molecules is determined from its molar ratio to Li^+ ions [Tsunekawa, Narumi, Sano, Hiwara, Fujita, and Yokoyama (2003)]. N_{Li}, N_{PC}, and Ω are listed in Table 1.

Before carrying out MD sampling, each system is equilibrated via several pro-

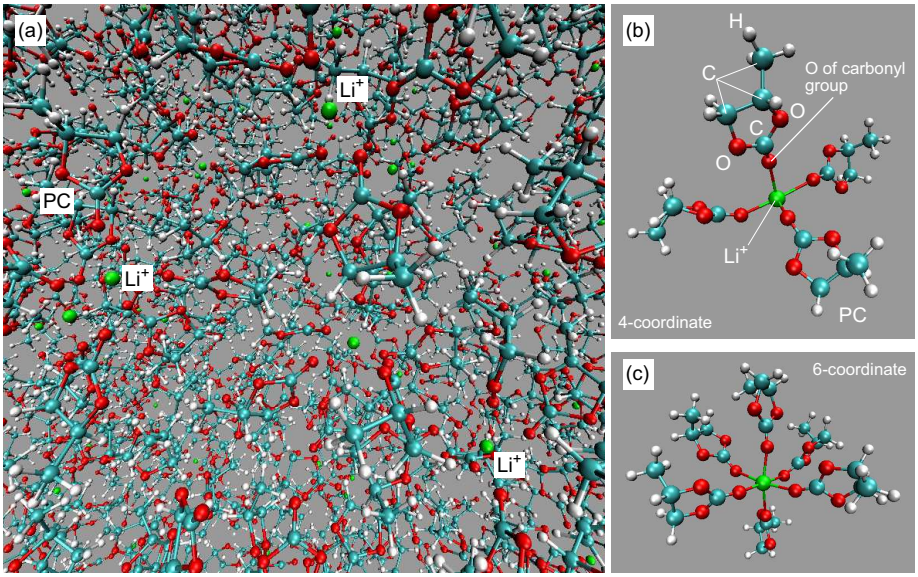

Figure 2: Schematic illustrations of (a) Li^+ ions in PC solvent at $c = 1.08 \times 10^3$ mol/m^3, (b) 4-coordinate and (c) 6-coordinate solvation structures, which can be observed in three-dimensional MD simulations.

Table 1: Number of molecules and atoms in each cell volume according to concentration c of Li^+ ions.

Li^+ concentration c [mol/m^3] (molar ratio of PC/Li^+)*		Number of molecules		Number of atoms N_a	Cell volume Ω [m^3]
		PC (N_{PC})	Li^+ (N_{Li})		
1.08 $\times 10^3$	(11.2)	560	50	7330	76995 $\times 10^{-30}$
1.63	(7.38)	369	50	4847	51082
2.05	(5.90)	295	50	3885	40404

*The molar ratio is referred to previous experiments by Tsunekawa et al. [Tsunekawa, Narumi, Sano, Hiwara, Fujita, and Yokoyama (2003)]. Note that the salt concentration in the experiment is assumed to be equal to c in the present study.

cesses. At first, under the constant N_{Li} and N_{PC}, constant Ω, and constant temperature T (NVT ensemble), the system is equilibrated at $T = 298$ K. Here, the Langevin thermostat is employed to control the isothermal condition. This process is performed for 10 ps. Next, under constant N_{Li} and N_{PC}, constant pressure P of 1.0×10^5 Pa, and constant T (NPT ensemble), the system is equilibrated for the duration of 100 ps for its suitable condition of c, as shown in Table 1. That is, equilibrium states at $c = 1.08 \times 10^3$, 1.63×10^3, and 2.05×10^3 mol/m^3 are attained after the two pre-processes above. After that, data sampling is carried

out during 100 ns under the condition of constant N_{Li} and N_{PC}, constant Ω, and constant energy E (NVE ensemble) [Hanasaki, Yonebayashi, and Kawano (2009); Hanasaki, Walther, Kawano, and Koumoutsakos (2010)]. In the simulations, the time step is set to 2.0 fs. In these computations, the particle mesh Ewald method for three-dimensional periodic boundary condition is applied with homogeneous neutralizing background charge [Hummer, Pratt, and García (1998)]. Although such a method may not be acceptable for energetical discussion, we focus only on the solvation structures in highly polarized conditions following previous studies [Lee and Rasaiah (1994); Koneshan, Rasaiah, Lynden-Bell, and Lee (1998)]. The computational conditions are determined on the basis of our previous studies [Kawano (1998); Nagahiro, Kawano, and Kotera (2007); Hanasaki, Haga, and Kawano (2008); Hanasaki, Shintaku, Matsunami, and Kawano (2009); Doi, Haga, Shintaku, and Kawano (2010); Doi, Uemura, and Kawano (2011)]. Furthermore, five independent runs for each c are carried out to obtain the average of simulation results. The force on ions is derived from spatial derivative of potential functions in which intramolecular and intermolecular interactions are considered [D. A. Case et al. (2008)]. The intramolecular interaction depends on bond lengths, bond angles, and dihedral angles in molecular structures. In addition, the intermolecular interaction includes the van der Waals (VDW) interaction and Coulomb interaction. The cut off radius of these non-contact interactions is set to 10.0×10^{-10} m [Hanasaki, Haga, and Kawano (2008); Hanasaki, Shintaku, Matsunami, and Kawano (2009); Doi, Haga, Shintaku, and Kawano (2010); Doi, Uemura, and Kawano (2011)].

Based on the computational results, solvation shells around Li^+ ions are analyzed in terms of the radial distribution function (RDF), diffusion coefficient, and coordination number. RDF is often used to evaluate the local concentration of molecules around a target particle, which is defined by the use of distance r measured from a Li^+ ion, such that

$$g_i(r) = \frac{\mathrm{d}n_i(r)}{4\pi\rho_i r^2 \mathrm{d}r}, \quad i = \mathrm{PC} \ \text{ or } \ \mathrm{Li}, \tag{17}$$

where $\mathrm{d}n_i(r)$ is the number of the ith species in a spherical shell at the radius r with the thickness of $\mathrm{d}r = 0.10 \times 10^{-10}$ m. $g_i(r)$ approaches 1 as $r \to \infty$. For PC solvent, ρ_{PC} is 7.11×10^{27} m^{-3} at 298 K [Jansen and Yeager (1973); Ue (1994)]. On the other hand, ρ_{Li} is defined as $50/\Omega$ in each c assuming the uniform distribution. In addition, the number of solvent molecules in a sphere of radius r can be estimated by the integral of $\mathrm{d}n_i(r)$ from 0 up to r:

$$n_i(r) = 4\pi\rho_i \int_0^r g_i(r') r'^2 \mathrm{d}r', \quad i = \mathrm{PC} \ \text{ or } \ \mathrm{Li}. \tag{18}$$

The coordination number associated with the solvation shells is defined for a characteristic radius. Evaluating $g_{\mathrm{PC}}(r)$ and $n_{\mathrm{PC}}(r)$ around Li^+ by Eq. 17 and Eq. 18,

the solvation shell structures must be clarified in detail. The MD sampling is expected to capture the maximum peaks of $g_i(r)$ that corresponds to the first and the other solvation shells [Tsunekawa, Narumi, Sano, Hiwara, Fujita, and Yokoyama (2003); Lee and Rasaiah (1994); Soetens, Millot, and Maigret (1998); Li and Balbuena (1999)]. Furthermore, effects of the solvation shells on the motion of Li^+ ions are investigated by evaluating D_{Li}, which can be obtained from the mean square displacement (MSD) in the limit of $t \to \infty$, according to the Einstein relation:

$$D_{Li} = \lim_{t\to\infty} \frac{1}{6t} \left\langle |\mathbf{r}(t) - \mathbf{r}(0)|^2 \right\rangle, \tag{19}$$

where $\mathbf{r}(t)$ denotes a position vector of Li^+ ions. The bracket in Eq. 19 means the ensemble average as follows:

$$\left\langle |\mathbf{r}(t) - \mathbf{r}(0)|^2 \right\rangle = \frac{1}{N_s N_{Li}} \sum_{j=1}^{N_s} \sum_{i=1}^{N_{Li}} \left| \mathbf{r}_i(t+t_j) - \mathbf{r}_i(t_j) \right|^2, \tag{20}$$

where N_s and N_{Li} $(= 50)$ are the number of time steps and that of Li^+ ions, respectively. N_s is set to 2.5×10^7, maintaining enough accuracy for the long time simulations [Doi, Uemura, and Kawano (2011)].

3 Results and Discussion

3.1 Distribution function g_{PC} and coordination number n_{PC} of PC

Resulting from the MD simulation, the number of PC molecules bonded with Li^+ was found to be 4–6, as shown in Fig. 2. Such molecular structures agree well with the experimental investigations [Kondo, Sano, Hiwara, Omi, Fujita, Kuwae, Iida, Mogi, and Yokoyama (2000)]. That is, the present MD simulation is valid to represent the conditions of Li^+ in PC solvent. Figure 3 shows $g_{PC}(r)$ and $n_{PC}(r)$ as a function of distance r between a Li^+ ion and a O atom of the carbonyl group in PC. Usually, the existence of solvation shells was confirmed with a peak of $g_{PC}(r)$, and the radius of the shell was determined from a minimum point just behind the maximum peak. The coordination number was defined as the number of molecules in the solvation shell. The conventional method is applied to estimate the coordination number [Lee and Rasaiah (1994); Doi, Uemura, and Kawano (2011)]. In Table 2, the first maximum, the first minimum, and the second maximum peaks of $g_{PC}(r)$ are presented by r_0, r_1, and r_2, respectively. The values of $g_{PC}(r_0)$, $n_{PC}(r_1)$, and $g_{PC}(r_2)$ are also listed in Table 2. The peaks of $g_{PC}(r_0)$ and $g_{PC}(r_2)$ indicate the first and the second solvation shells, respectively. It was also confirmed from Fig. 3 that $g_{PC}(r)$ converged to 1 as $r \to \infty$. In the case of $c = 1.08 \times 10^3$ mol/m^3

as shown in Fig. 3(a), the first and the second maximum peaks were observed at $r_0 = 2.05 \times 10^{-10}$ and $r_2 = 8.39 \times 10^{-10}$ m, respectively. In particular, $g_{\mathrm{PC}}(r_0)$ was prominent compared with the other peaks. This means that solvent molecules were highly concentrated in the first shell. The second shell indicated by r_2 was also clearly observed, as shown in the magnified views inserted in Fig. 3. As demonstrated in Fig. 3(a), a drastic increase in the coordination number was observed near the first peak at $r_0 = 2.05 \times 10^{-10}$ m. The coordination number was estimated by the integral from 0 to the minimum peak at $r_1 = 3.47 \times 10^{-10}$ m according to Eq. 18. In the case of $c = 1.08 \times 10^3$ mol/m^3, $n_{\mathrm{PC}}(r_1)$ was evaluated as 5.37. That is, Li^+ ions move with this number of PC molecules that play roles of the additional mass and the larger equivalent radius of Li^+ complex. According to some experimental results that suggested the coordination number more than 4[Saito, Yamamoto, Nakamura, Kageyama, Ishikawa, Miyoshi, and Matsuoka (1999); Kondo, Sano, Hiwara, Omi, Fujita, Kuwae, Iida, Mogi, and Yokoyama (2000)], the present result is valid to simulate a typical condition in the real system. The similar tendency was also obtained in the case of $c = 1.63 \times 10^3$ mol/m^3 as shown in Fig. 3(b). From this result, the first and the second maximum peaks of $g_{\mathrm{PC}}(r)$ were observed at $r_0 = 2.00 \times 10^{-10}$ and $r_2 = 8.45 \times 10^{-10}$ m, respectively, and $n_{\mathrm{PC}}(r_1)$ was evaluated as 5.09. The values of $g_{\mathrm{PC}}(r)$ and $n_{\mathrm{PC}}(r)$ in the case of $c = 2.05 \times 10^3$ mol/m^3 are shown in Fig. 3(c). The peaks were obtained at $r_0 = 2.00 \times 10^{-10}$ and $r_2 = 8.50 \times 10^{-10}$ m, and $n_{\mathrm{PC}}(r_1)$ resulted in 4.96.

In these three cases, r_0 was almost constant regardless of c, since some solvent molecules were tightly bound by a Li^+ ion in the first solvation shell and the bond length was not affected by c. On the other hand, r_2, which indicates the second solvation shell, tended to become larger with increasing c. This result suggests that solvent molecules in the second solvation shell seem to be attracted by more than one Li^+ ion due to the high concentrations and that the distribution of PC molecules tends to be extended. In addition, $n_{\mathrm{PC}}(r_1)$ tended to slightly decrease with increase in c. It may be said that some solvent molecules near the edge of the first shell shift to the second shell. In the case of $c = 1.08 \times 10^3$ mol/m^3, according to $n_{\mathrm{PC}}(r_1)$ of 5.37 and 50 Li^+ ions in the computational cell volume employed in this study, it was simply estimated that 269 ($= 5.37 \times 50$) PC molecules contributed to the first solvation shell. That is, the ratio of 269 PC molecules to the total number of $N_{\mathrm{PC}} = 560$ in the computational cell was 0.48 ($= 269/560$). Similarly, the ratios for $c = 1.63 \times 10^3$ and 2.05×10^3 mol/m^3 were evaluated as 0.69 and 0.84, respectively. These three values of 0.48, 0.69, and 0.84 are almost proportional to c, as shown in Table 3. The number of PC molecules that contributed to the first solvation shell proportionally increased with the number of Li^+ ions, but overlaps between the first shells were not observed, since the count of PC molecules that were in the first

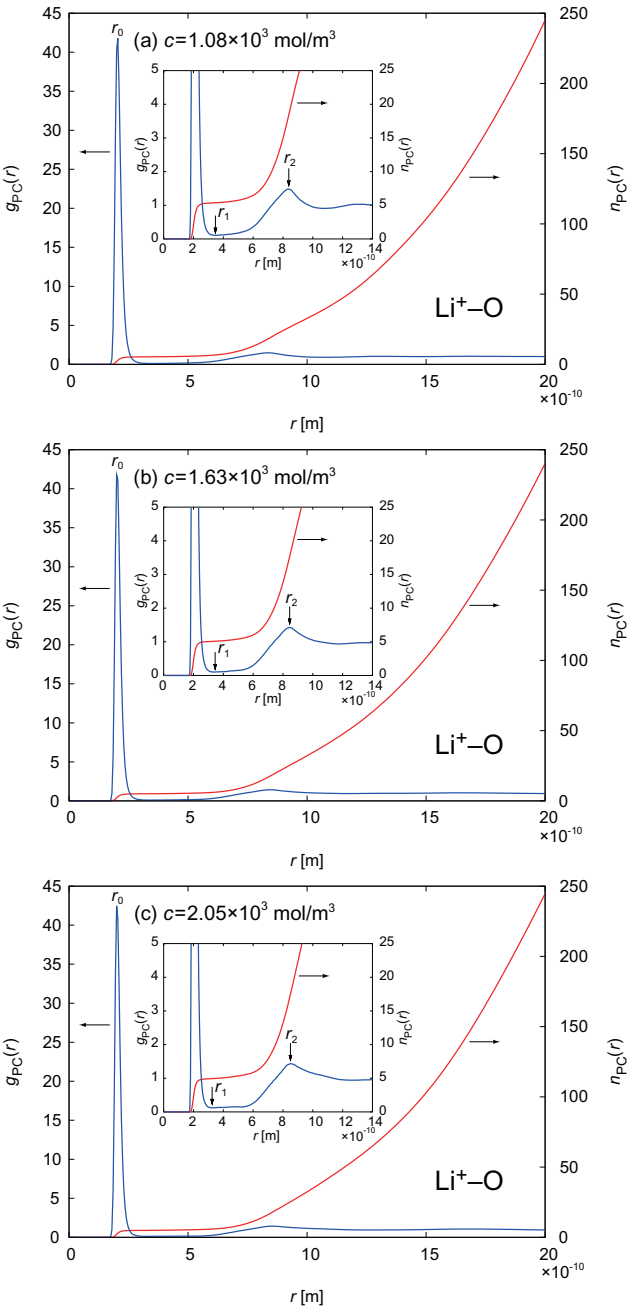

Figure 3: Radial distribution function $g_{\mathrm{PC}}(r)$ and the number $n_{\mathrm{PC}}(r)$ of PC molecules as a function of distance r between a Li^+ ion and a O atom of the carbonyl group in PC for $c = 1.08 \times 10^3$, 1.63×10^3, and 2.05×10^3 mol/m^3; magnified views are presented in insets.

Table 2: Radial distribution function g_{PC} and coordination number n_{PC} of the first and the second shells; r_0, r_1, and r_2 denote the first maximum, the first minimum, and the second maximum peaks of g_{PC} shown in Fig. 3, respectively.

c [mol/m^3]	r_0 [m]	$g_{\mathrm{PC}}(r_0)$	r_1 [m]	$n_{\mathrm{PC}}(r_1)$	r_2 [m]	$g_{\mathrm{PC}}(r_2)$
1.08×10^3	$2.05 \pm 0.00 \times 10^{-10}$	41.69 ± 0.26	$3.47 \pm 0.08 \times 10^{-10}$	5.37 ± 0.01	$8.39 \pm 0.02 \times 10^{-10}$	1.48 ± 0.01
1.63	2.00 ± 0.00	41.70 ± 0.06	3.45 ± 0.08	5.09 ± 0.01	8.45 ± 0.04	1.42 ± 0.01
2.05	2.00 ± 0.00	42.70 ± 0.17	3.25 ± 0.09	4.96 ± 0.02	8.50 ± 0.00	1.44 ± 0.01

shell and occupied by multiple Li^+ ions was almost zero. In addition, the smallest length of the computational cells was larger than twice of the largest radius of the second solvation shell ($r_2 = 8.50 \times 10^{-10}$ m). Thus, the first solvation shells were clearly isolated with each other. In each condition, solvent PC molecules in the first shell were not occupied simultaneously by more than one Li^+ ion.

In the same manner, the number of PC molecules simultaneously occupied by two or more Li^+ ions in the second solvation shells were counted. PC molecules in the overlapped regions between Li^+ ions were observed and counted from the MD results. Edges of the second shells were not so clear that the number of them in the second shell was estimated by integrating up to $r_2 = 8.39 \times 10^{-10}$, 8.45×10^{-10}, and 8.50×10^{-10} m for $c = 1.08 \times 10^3$, 1.63×10^3, and 2.05×10^3 mol/m^3, respectively. Then, multiply-counted PC molecules were regarded as shared ones by more than one Li^+ ion. As a result, the number was evaluated as 293 ± 6, 298 ± 4, and 274 ± 1 for $c = 1.08 \times 10^3$, 1.63×10^3, and 2.05×10^3 mol/m^3, respectively, and the ratio to N_{PC} was 0.52, 0.81, and 0.93, respectively, as summarized in Table 3.

3.2 *Distribution function g_{Li} and coordination number n_{Li} of Li^+*

Figure 4 shows $g_{\mathrm{Li}}(r)$ and $n_{\mathrm{Li}}(r)$ with respect to the Li^+–Li^+ interaction. It was found that $g_{\mathrm{Li}}(r)$ exhibited several peaks that appeared at almost the same distance in each c. In particular, the most prominent peak was observed near $r_p = 9.13 \times 10^{-10}$ m. It is suggested that Li^+ ions tend to be located at the constant distance regardless of c. The peak value of $g_{\mathrm{Li}}(r)$ at r_{p} was 1.80, 1.91, and 2.00 for $c = 1.08 \times 10^3$, 1.63×10^3, and 2.05×10^3 mol/m^3, respectively. Then, $n_{\mathrm{Li}}(r)$ evaluated at the minimum point $r_{\mathrm{p}'}$ of $g_{\mathrm{Li}}(r)$ behind r_{p} was 3.79, 6.17, and 8.18, respectively, and they were in proportion to c in this range. These values are also summarized in Table 3. This result indicates that Li^+ ions in PC solvent tend to attractively interact with each other due to the overlap of their second solvation shells rather than the uniform distribution in the solution. As expressed by schematic illustrations in Fig. 5, the discussion above clarifies multiply-occupied PC molecules and attractive interactions between solvation shells with increase in c. On the other hand, the MD results do not mean that Li^+ ions strongly aggregate to form rigid crystal-like structures. The motion of Li^+ ions appeared to be induced by collisions with surrounding PC molecules and showed linearity in the MSDs. In addition, a very small peak was observed at near 3.40×10^{-10} m, and this peak was considered to be caused by two Li^+ ions occasionally approaching each other to bond with a PC molecule, although this conformation was not conserved so long period due to repulsive interactions between them. In some experimental results [Saito, Yamamoto, Nakamura, Kageyama, Ishikawa, Miyoshi,

Table 3: Ratios of solvated PC molecules to N_{PC} in the first solvation shell and multiply-occupied ones in the second shell, and g_{Li} and n_{Li} at the most prominent peak r_{p} and at the minimum point $r_{\mathrm{p}'}$ just behind r_{p}, respectively.

c [mol/m^3]	Ratio of PC molecules to N_{PC}		Li^+–Li^+ interaction			
	1st solvation shell	multiply-occupied	r_{p} [m]	$g_{\mathrm{Li}}(r_{\mathrm{p}})$	$r_{\mathrm{p}'}$ [m]	$n_{\mathrm{Li}}(r_{\mathrm{p}'})$
1.08×10^3	0.48	0.52	9.13×10^{-10}	1.80	11.8×10^{-10}	3.79
1.63	0.69	0.81	9.11	1.91	11.8	6.17
2.05	0.84	0.93	9.14	2.00	11.8	8.18

and Matsuoka (1999); Kondo, Sano, Hiwara, Omi, Fujita, Kuwae, Iida, Mogi, and Yokoyama (2000); Zhao, Wang, He, Wan, and Jiang (2008)], the attractive interaction between Li^+ ions was certainly predicted, although the detailed mechanism has not yet been elucidated. The present numerical analysis qualitatively explains the fact in the experiments.

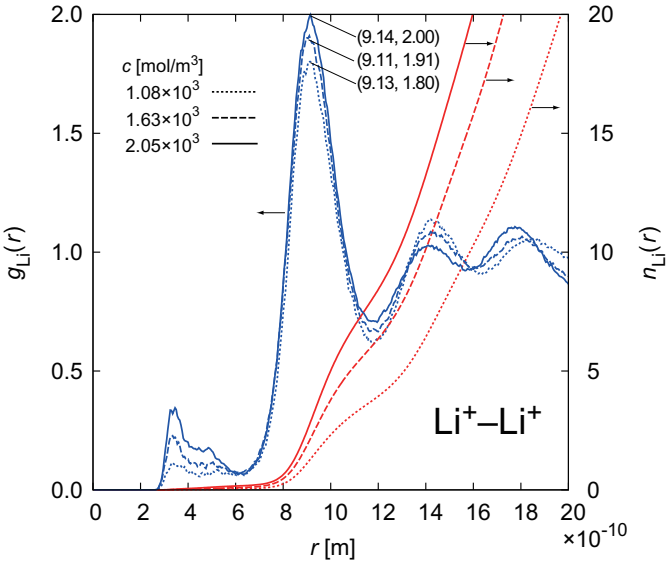

Figure 4: Radial distribution function $g_{\mathrm{Li}}(r)$ and the number $n_{\mathrm{Li}}(r)$ of Li^+ as a function of distance r between Li^+ions for $c = 1.08 \times 10^3$ (dotted line), 1.63×10^3 (dashed line), and 2.05×10^3 mol/m^3 (solid line).

3.3 Diffusion coefficient D_{Li} of Li^+

Figure 6 shows the MSDs of Li^+ ions computed from the five runs in the time range from 0 to 50 ns according to Eq. 20. The results are presented by solid lines and the linear least-squares fits are shown by dashed lines. In each concentration, the results showed small deviations from their linear fits. It was found that the MSDs tended to decrease with increase in c. According to the gradient of the linear fit, D_{Li} could be evaluated by Eq. 19. For $c = 1.08 \times 10^3$, 1.63×10^3, and 2.05×10^3 mol/m^3, D_{Li} resulted in $(7.49 \pm 0.36) \times 10^{-11}$, $(5.89 \pm 0.58) \times 10^{-11}$, and $(2.15 \pm 0.46) \times 10^{-11}$ m^2/s, respectively. A strong c dependency of D_{Li} was found similarly to a well-known experimental fact [Klassen, Aroca, Nazri, and Nazri (1998); Saito, Yamamoto, Nakamura, Kageyama, Ishikawa, Miyoshi, and Matsuoka (1999); Kondo,

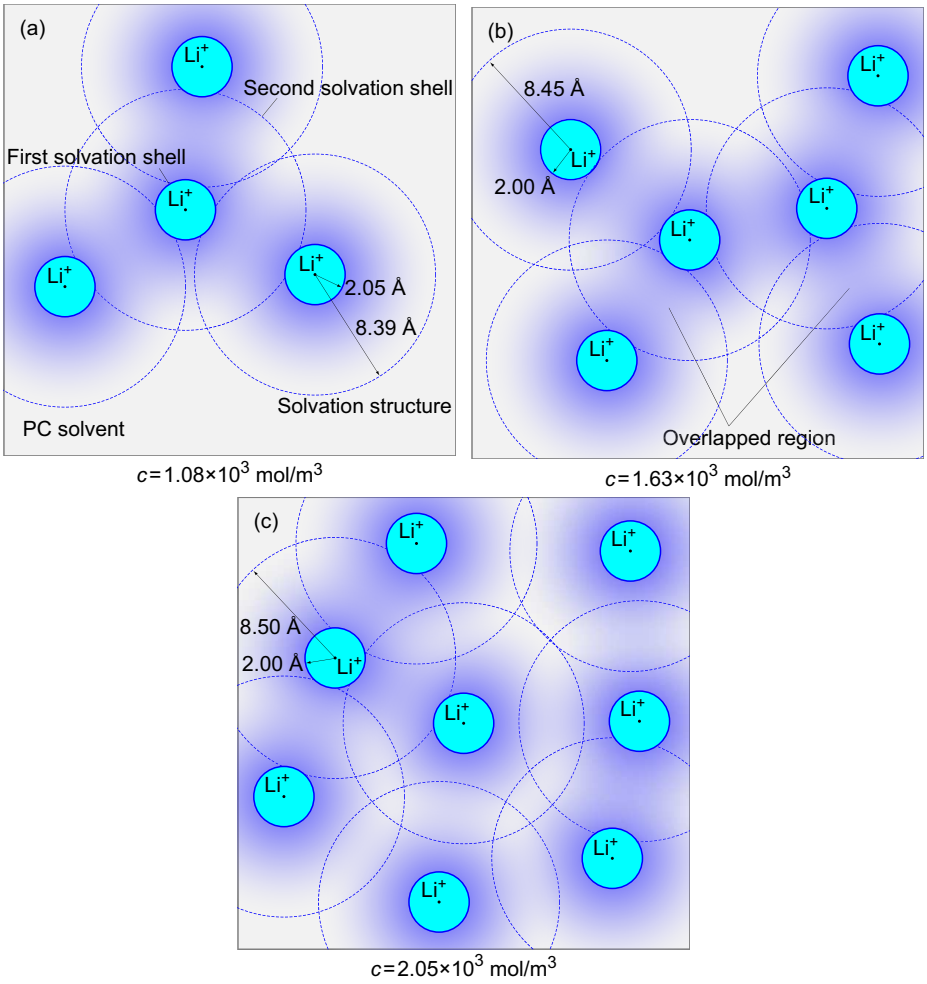

Figure 5: Schematic illustrations of solvation structures around Li^+ ions for (a) $c = 1.08 \times 10^3$ mol/m^3, (b) 1.63×10^3 mol/m^3, and (c) 2.05×10^3 mol/m^3. In overlapped regions of the second solvation shells, a PC molecule tends to be attracted by multiple Li^+ ions with increasing Li^+ concentrations.

Sano, Hiwara, Omi, Fujita, Kuwae, Iida, Mogi, and Yokoyama (2000); Aihara, Arai, and Hayamizu (2000); Tsunekawa, Narumi, Sano, Hiwara, Fujita, and Yokoyama (2003); Zhao, Wang, He, Wan, and Jiang (2008); Takeuchi, Kameda, Umebayashi, Ogawa, Sonoda, Ishiguro, Fujita, and Sano (2009)]. Resulting from the long period MD sampling with multiple runs, enough accuracy was maintained.

The validity of the numerical evaluation was also confirmed in our previous study [Doi, Uemura, and Kawano (2011)].

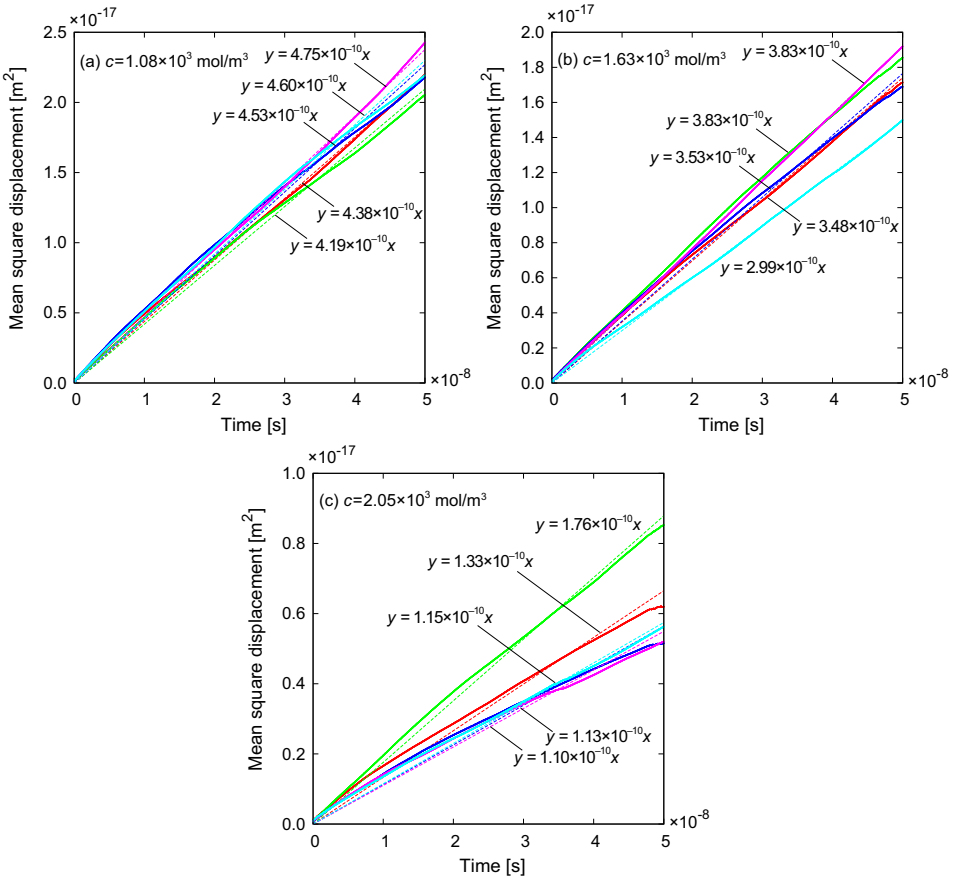

Figure 6: Mean square displacement of Li^+ ions in PC solvent for (a) $c = 1.08 \times 10^3$ mol/m^3, (b) 1.63×10^3 mol/m^3, and (c) 2.05×10^3 mol/m^3. MD results and linear least-squares fits for five runs are shown by solid and dashed lines, respectively.

In general, the diffusion coefficient obtained from the Brownian motions in free solution can be expressed by Eq. 16. For Li^+ ions, the diffusion coefficient was evaluated as $D^0_{Li} = 2.49 \times 10^{-10}$ m^2/s, according to $T = 298$ K, $\mu = 2.53 \times 10^{-3}$ Pa s, and $a = 3.47 \times 10^{-10}$ m in PC solvent that was the equivalent radius of the first solvation shell referring to r_1 at $c = 1.08 \times 10^3$ mol/m^3. The order of D^0_{Li} was in considerable agreement with the experimental data of 2.2×10^{-10} m^2/s for 0.1×10^3 mol/m^3 $LiBF_4$ in PC [Tsunekawa, Narumi, Sano, Hiwara, Fujita, and

Yokoyama (2003)] and that of 2.0×10^{-10} m^2/s for 0.1×10^3 mol/m^3 $LiPF_6$ in PC [Takeuchi, Kameda, Umebayashi, Ogawa, Sonoda, Ishiguro, Fujita, and Sano (2009)]. However, this coefficient does not predict the c dependency as far as μ and a are not affected by c.

Considering frictions via the second solvation shells, an additional term depending on c should be considered on the basis of the experimental data [Saito, Yamamoto, Nakamura, Kageyama, Ishikawa, Miyoshi, and Matsuoka (1999); Aihara, Arai, and Hayamizu (2000); Tsunekawa, Narumi, Sano, Hiwara, Fujita, and Yokoyama (2003)]. At first, Li^+ ions move interacting with polar solvent molecules and thus, the energy dissipation of solute ions can be represented by the Stokes drag: $6\pi\mu r_1\mathbf{u}$. Furthermore, as shown in Fig. 4, Li^+ ions appear to be stable at their constant distance approximately 9.13×10^{-10} m. The overlap of their second shells and $n_{\mathrm{Li}}(r_{\mathrm{p}'})$ increased in proportion to c as shown in Table 3. Thus, we suppose a model of $\sum_{j\neq i}\xi_{ij}$ as a function of c, such that $\sum_{j\neq i}\xi_{ij} \equiv \xi_0 V N_{\mathrm{A}} c$, where ξ_0 is the basic unit of the friction coefficient and $VN_{\mathrm{A}}c$ represents the coordination number of Li^+ ion with the characteristic volume V due to the second solvation shell. Including these components, D_{Li} resulted in

$$D_{\mathrm{Li}} = D^0_{\mathrm{Li}}\left(1+\frac{\sum_{j\neq i}\xi_{ij}}{6\pi\mu r_1}\right)^{-2} = 2.49\times10^{-10}\left(1+\frac{1.29\times10^{-14}}{1.65\times10^{-11}}c\right)^{-2}, \tag{21}$$

where the values of $6\pi\mu r_1$ and $\xi_0 V N_{\mathrm{A}}$ were determined by fitting Eq. 21 to the results from our MD simulations. As shown in Table 3, according to the equivalence between $VN_{\mathrm{A}}c$ and $n_{\mathrm{Li}}(r_{\mathrm{p}'}) = 3.79$ for $c = 1.08 \times 10^3$ mol/m^3, such that $VN_{\mathrm{A}}c = 3.79$, V and ξ_0 were evaluated as 5.83×10^{-27} m^3 and 3.68×10^{-12} kg/s, respectively. Here, although ξ_0 was treated as a fitting parameter, the hydrodynamic radius, evaluated by the equivalence of $\xi_0 = 6\pi\mu a$, resulted in $a = 7.72 \times 10^{-11}$ m. This value is near the ionic radius of Li^+ experimentally measured [Ashcroft and Mermin (1976); Meyer, Heinzelmann, Rudin, and Güntherodt (1990); Martínez-Juárez, Pecharromán, Iglesias, and Rojo (1998)]. Furthermore, a sphere radius evaluated from $V = 5.83 \times 10^{-27}$ m^3 corresponds to 11.2×10^{-10} m and this value is very near to $r_{\mathrm{p}'} = 11.8 \times 10^{-10}$ m as shown in Table. 3. Thus, the value of V actually indicates the volume of the second solvation shell due to the attractive interactions between Li^+ ions. Consequently, the theoretical evaluation was found to be valid to represent the diffusivity caused by the effects of the first and the second solvation shells.

Figure 7 shows plots of the theoretical prediction and the present MD data in comparison with the experimental results [Saito, Yamamoto, Nakamura, Kageyama, Ishikawa, Miyoshi, and Matsuoka (1999); Aihara, Arai, and Hayamizu (2000); Tsunekawa, Narumi, Sano, Hiwara, Fujita, and Yokoyama (2003)]. Lithium salt

concentrations in the experiments corresponded to c in the present MD simulation in which Li^+ was assumed to be fully-separated from its counter anion. Resulting from decrease in D_{Li} as a function of c, it is clearly indicated that the solvation effect on D_{Li} becomes prominent as c increases as shown by the solid line in Fig. 7. This characteristics cannot be represented by only the constant Stokes drag.

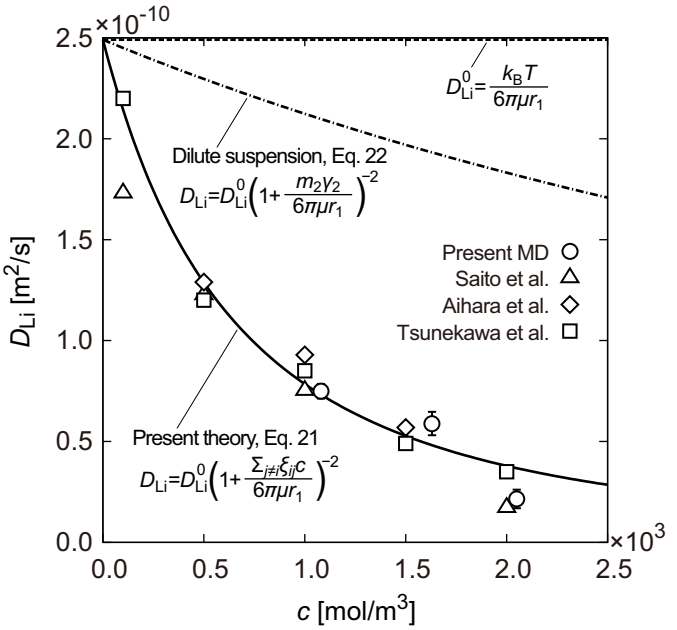

Figure 7: Comparison of D_{Li} between the present MD result (○) which assumes the fully-ionized condition of lithium salt and experimental data by Saito et al. [Saito, Yamamoto, Nakamura, Kageyama, Ishikawa, Miyoshi, and Matsuoka (1999)] (△), Aihara et al. [Aihara, Arai, and Hayamizu (2000)] (◇), and Tsunekawa et al. [Tsunekawa, Narumi, Sano, Hiwara, Fujita, and Yokoyama (2003)] (□). The present theoretical analysis using Eq. 21 is shown by solid line, where D^0_{Li} due to Stokes drag without c dependency is by dashed line and another theoretical line from collisions of the second solvation shells in dilute suspension (Eq. 22) is by dashed-dotted line.

For comparison, assuming collisions of the second solvation shells in dilute suspension, the friction force was calculated by the use of the collision frequency $\gamma_2 = \langle|\mathbf{u}|\rangle / \lambda_2$ with the mean free path λ_2 and the mass m_2 of the second solvation shell, such that $m_2\gamma_2\mathbf{u}$. In this model, collisions between the rigid bodies were only taken into account. Referring to the case of $c = 1.08 \times 10^3$ mol/m^3,

these values were determined as follows: $m_2 = 3.15 \times 10^{-24}$ kg for $n_{\mathrm{PC}}(r_2) = 18.5$, $\lambda_2 = 1/\left(\sqrt{2}\pi {d_2}^2 N_{\mathrm{A}} c\right) = 1/\left(7.53 \times 10^6 c\right)$ m, where $d_2 = 1.68 \times 10^{-9}$ m was the diameter of the second solvation shell, and $\langle|\mathbf{u}|\rangle = \sqrt{8k_{\mathrm{B}}T/(m_2\pi)} = 57.7$ m/s [Vincenti and Kruger Jr. (1965)]. As a result, the friction force was evaluated as $m_2\gamma_2\mathbf{u} = 1.37 \times 10^{-15} c\mathbf{u}$. This value seems to be one order of magnitude smaller than the corresponding term in Eq. 21, such that $\xi_0 V N_{\mathrm{A}} c\mathbf{u} = 1.29 \times 10^{-14} c\mathbf{u}$. The theoretical line of D_{Li} by replacing $\xi_0 V N_{\mathrm{A}} c\mathbf{u}$ in Eq. 21 with $m_2\gamma_2\mathbf{u}$ is also presented by the dashed-dotted line in Fig. 7, such that

$$D_{\mathrm{Li}} = D^0_{\mathrm{Li}} \left(1 + \frac{m_2\gamma_2}{6\pi\mu r_1}\right)^{-2} = 2.49 \times 10^{-10} \left(1 + \frac{1.37 \times 10^{-15}}{1.65 \times 10^{-11}} c\right)^{-2}. \tag{22}$$

Resulting from the discussion above, it is supposed that the energy dissipation via the multiply-occupied PC molecules in the second solvation shells causes the drastic reduction of D_{Li}. This is a reason why D_{Li} strongly depends on c. On the other hand, a disagreement also becomes apparent when c becomes higher than 2.0×10^3 mol/m^3. It is suspected that ion pairs of Li^+ and its counter anion also cause to reduce D_{Li} at high c regions [Takeuchi, Kameda, Umebayashi, Ogawa, Sonoda, Ishiguro, Fujita, and Sano (2009)], which has not been taken into account in our theoretical model. According to the assumption of $\sum_{j\neq i} \xi_{ij} \ll m_i\gamma_i$, the theoretical validity of c may be limited at most 1.28×10^3 mol/m^3. Consideration of higher order terms in Eq. 13 is expected to improve the quantitative agreement in the wider range of c. In experimental results [Saito, Yamamoto, Nakamura, Kageyama, Ishikawa, Miyoshi, and Matsuoka (1999); Aihara, Arai, and Hayamizu (2000); Tsunekawa, Narumi, Sano, Hiwara, Fujita, and Yokoyama (2003); Zhao, Wang, He, Wan, and Jiang (2008)], more complicated solvation structures were also predicted. In our future plan, a course graining procedure [Nagahiro, Kawano, and Kotera (2007); Doi, Haga, Shintaku, and Kawano (2010)] will be applied to MD simulations in order to treat the complicated and large molecular systems. This study focusing on the solvation shells around Li^+ ions have indicated some important results about ion transport phenomena not only in a lithium salt solution but also in various electrolyte solutions.

4 Conclusions

In the present study, focusing on solvation structures of Li^+ ions in PC solvent, an ion transport phenomenon was modeled based on the Langevin equation, and was simulated using MD simulations. The MD results for the concentration of Li^+ ions ranging from $c = 1.08 \times 10^3$ to 2.05×10^3 mol/m^3 were analyzed in terms of the

radial distribution function, coordination number, and diffusion coefficient. Several important results could be obtained as follows:

1. Resulting from the MD simulations, the coordination number analysis quantitatively clarified the solvation numbers from 4 to 6, which was predicted in the experimental results by the other researchers [Saito, Yamamoto, Nakamura, Kageyama, Ishikawa, Miyoshi, and Matsuoka (1999); Kondo, Sano, Hiwara, Omi, Fujita, Kuwae, Iida, Mogi, and Yokoyama (2000)].

2. The existence of the second solvation shell was confirmed by the radial distribution function analysis. It was found that overlaps of the second shells became prominent at high salt concentrations and that the solvation shells interacted attractively with each other via the multiply-occupied PC molecules.

3. A well-known experimental fact that D_{Li} drastically decreased with increasing c [Saito, Yamamoto, Nakamura, Kageyama, Ishikawa, Miyoshi, and Matsuoka (1999); Aihara, Arai, and Hayamizu (2000); Tsunekawa, Narumi, Sano, Hiwara, Fujita, and Yokoyama (2003); Zhao, Wang, He, Wan, and Jiang (2008)] was elucidated by both the MD simulations and the theoretical model based on the Langevin equation. The solvation effects on the decrease in D_{Li} could be clarified not only by the hydrodynamic radius of the first solvation shell, but also by the c-dependent frictions due to the second solvation shell.

References

Aihara, Y.; Arai, S.; Hayamizu, K. (2000): Ionic conductivity, DSC and self diffusion coefficients of lithium, anion, polymer, and solvent of polymer gel electrolytes: the structure of the gels and the diffusion mechanism of the ions. *Electrochim. Acta*, vol. 45, pp. 1321–1326.

Aricò, A. S.; Bruce, P.; Scrosati, B.; Tarascon, J.; Schalkwijk, W. V. (2005): Nanostructured materials for advanced energy conversion and storage devices. *Nat. Mater.*, vol. 4, pp. 366–377.

Arora, P.; Doyle, M.; Gozdz, A. S.; White, R. E.; Newman, J. (2000): Comparison between computer simulations and experimental data for high-rate discharges of plastic lithium-ion batteries. *J. Power Sources*, vol. 88, pp. 219–231.

Ashcroft, N. W.; Mermin, N. D. (1976): *Solid State Physics*. Thomson Leaning, Inc.

Barbero, G.; Evangelista, L. R.; Lelidis, I. (2006): Ionic contribution to the electric current in an electrolytic cell submitted to an external voltage. *Phys. Rev. E*, vol. 74, pp. 022501–1–022501–4.

Barbero, G.; Lelidis, I. (2007): Evidence of the ambipolar diffusion in the impedance spectroscopy of an electrolytic cell. *Phys. Rev. E*, vol. 76, pp. 051501–1–051501–9.

Costa, L. T.; Ribeiro, M. C. C. (2007): Molecular dynamics simulation of polymer electrolytes based on poly(ethylene oxide) and ionic liquids. ii. dynamical properties. *J. Chem. Phys.*, vol. 127, pp. 164901–1–164901–7.

D. A. Case et al. (2008): *computer code* AMBER 10. University of California, San Francisco.

Doi, K.; Haga, T.; Shintaku, H.; Kawano, S. (2010): Developments of coarse graining DNA models for single nucleotide resolution analysis. *Phil. Trans. R. Soc. A*, vol. 368, pp. 2615–2628.

Doi, K.; Nakano, H.; Ohta, H.; Tachibana, A. (2007): First-principle molecular-dynamics study of hydrogen and aluminum nanowires in carbon nanotubes. *Mater. Sci. Forum*, vol. 539–543, pp. 1409–1414.

Doi, K.; Onishi, I.; Kawano, S. (2011): *Ab initio* molecular dynamics of H_2 dissociative adsorption on graphene surfaces. *Comput. Model. Eng. Sci.*, vol. 77, pp. 113–136.

Doi, K.; Onishi, I.; Kawano, S. (2012): Dissociative adsorption of H_2 molecules on steric graphene surface: *Ab initio* MD study based on DFT. *Comput. Theor. Chem.*, vol. 994, pp. 54–64.

Doi, K.; Takeuchi, H.; Nii, R.; Akamatsu, S.; Kakizaki, T.; Kawano, S. (2013): Self-assembly of 50 bp poly(dA)·poly(dT) DNA on highly oriented pyrolytic graphite via atomic force microscopy observation and molecular dynamics simulation. *J. Chem. Phys.*, vol. 139, pp. 085102–1–085102–10.

Doi, K.; Toyokita, Y.; Akamatsu, S.; Kawano, S. (2014): Reaction–diffusion wave model for self-assembled network formation of poly(dA)·poly(dT) DNA on mica and HOPG surfaces. *Comput. Methods Biomech. Biomed. Eng.*, vol. 17, pp. 661–667.

Doi, K.; Tsutsui, M.; Ohshiro, T.; Chien, C.-C.; Zwolak, M.; Taniguchi, M.; Kawai, T.; Kawano, S.; Di Ventra, M. (2014): Nonequilibrium ionic response of biased mechanically controllable break junction (MCBJ) electrodes. *J. Phys. Chem. C*, vol. 118, pp. 3758–3765.

Doi, K.; Ueda, M.; Kawano, S. (2011): Theoretical model of nanoparticle detection mechanism in microchannel with gating probe electrodes. *J. Comput. Sci. Technol.*, vol. 5, pp. 78–88.

Doi, K.; Uemura, T.; Kawano, S. (2011): Molecular dynamics study of solvation effect on diffusivity changes of DNA fragments. *J. Mol. Model.*, vol. 17, pp. 1457–1465.

Doi, K.; Yoshida, K.; Nakano, H.; Tachibana, A.; Tabata, T.; Kojima, Y.; Okazaki, K. (2005): *Ab initio* calculation of electron effective masses in solid pentacene. *J. Appl. Phys.*, vol. 98, pp. 113709–1–113709–7.

Hamad, I. A.; Novotny, M. A.; Wipf, D. O.; Rikvold, P. A. (2010): A new battery-charging method suggested by molecular dynamics simulations. *Phys. Chem. Chem. Phys.*, vol. 12, pp. 2740–2743.

Hanasaki, I.; Haga, T.; Kawano, S. (2008): The antigen-antibody unbinding process through steered molecular dynamics of a complex of an Fv fragment and lysozyme. *J. Phys.: Condens. Matter.*, vol. 20, pp. 255238–1–255238–10.

Hanasaki, I.; Shintaku, H.; Matsunami, S.; Kawano, S. (2009): Structural and tensile properties of self-assembled DNA network on mica surface. *Comput. Model. Eng. Sci.*, vol. 46, pp. 191–207.

Hanasaki, I.; Walther, J. H.; Kawano, S.; Koumoutsakos, P. (2010): Coarse-grained molecular dynamics simulations of shear-induced instabilities of lipid bilayer membranes in water. *Phys. Rev. E.*, vol. 82, pp. 051602–1–051602–6.

Hanasaki, I.; Yonebayashi, T.; Kawano, S. (2009): Molecular dynamics of a water jet from a carbon nanotube. *Phys. Rev. E.*, vol. 79, pp. 046307–1–046307–7.

Hummer, G.; Pratt, L. R.; García, A. E. (1998): Molecular theories and simulation of ions and polar molecules in water. *J. Phys. Chem. A*, vol. 102, pp. 7885–7895.

Jansen, M. L.; Yeager, H. L. (1973): A conductance study of 1–1 electrolytes in propylene carbonate. *J. Phys. Chem.*, vol. 77, pp. 3089–3092.

Kawano, S. (1998): Molecular dynamics of rupture phenomena in a liquid thread. *Phys. Rev. E*, vol. 58, pp. 4468–4472.

Kawano, S.; Nishimura, F. (2005): Numerical analysis of discharge characteristics in lithium ion batteries using multiphase fluids model. *Jpn. J. Appl. Phys.*, vol. 44, pp. 4218–4228.

Kawano, S.; Nishimura, F. (2005): Numerical analysis on charge characteristics in lithium ion batteries by multiphase fluids model. *JSME. Int. J., Ser. B*, vol. 48, pp. 548–554.

Kawano, S.; Nishimura, F. (2008): Electrochemical–thermal analysis of lithium ion batteries based on multiphase fluids model. *Int. J. Transp. Phenom.*, vol. 10, pp. 93–101.

Klassen, B.; Aroca, R.; Nazri, M.; Nazri, G. A. (1998): Raman spectra and transport properties of lithium perchlorate in ethylene carbonate based binary solvent systems for lithium batteries. *J. Phys. Chem. B*, vol. 102, pp. 4795–4801.

Kondo, K.; Sano, M.; Hiwara, A.; Omi, T.; Fujita, M.; Kuwae, A.; Iida, M.; Mogi, K.; Yokoyama, H. (2000): Conductivity and solvation of Li^+ ions of $LiPF_6$ in propylene carbonate solutions. *J. Phys. Chem. B*, vol. 104, pp. 5040–5044.

Koneshan, S.; Rasaiah, J. C.; Lynden-Bell, R. M.; Lee, S. H. (1998): Solvent structure, dynamics, and ion mobility in aqueous solutions at 25 °C. *J. Phys. Chem. B*, vol. 102, pp. 4193–4204.

Lee, S. H.; Rasaiah, J. C. (1994): Molecular dynamics simulation of ionic mobility. i. alkali metal cations in water at 25 °C. *J. Chem. Phys.*, vol. 8, pp. 6964–6974.

Li, T.; Balbuena, P. B. (1999): Theoretical studies of lithium perchlorate in ethylene carbonate, propylene carbonate, and their mixtures. *J. Electrochem. Soc.*, vol. 164, pp. 3613–3622.

Martínez-Juárez, A.; Pecharromán, C.; Iglesias, J. E.; Rojo, J. M. (1998): Relationship between activation energy and bottleneck size for Li^+ ion conduction in NASICON materials of composition $LiMM'(PO_4)_3$; M, M' = Ge, Ti, Sn, Hf. *J. Phys. Chem. B*, vol. 102, pp. 372–375.

McQuarrie, D. A. (2000): *Statistical Mechanics*. University Science Books, Sausalito, California.

Meyer, E.; Heinzelmann, H.; Rudin, H.; Güntherodt, H.-J. (1990): Atomic resolution on LiF (001) by atomic force microscopy. *Z. Phys. B*, vol. 79, pp. 3–4.

Nagahiro, S.; Kawano, S.; Kotera, H. (2007): Separation of long DNA chains using a nonuniform electric field: A numerical study. *Phys. Rev. E*, vol. 75, pp. 011902–1–011902–5.

Nakano, H.; Ohta, H.; Yokoe, A.; Doi, K.; Tachibana, A. (2006): First-principle molecular-dynamics study of hydrogen adsorption on an aluminum-doped carbon nanotube. *J. Power Sources*, vol. 163, pp. 125–134.

Newman, J.; Thomas, K. E.; Hafezi, H.; Wheeler, D. R. (2003): Modeling of lithium-ion batteries. *J. Power Sources*, vol. 119–121, pp. 838–843.

Saito, Y.; Yamamoto, H.; Nakamura, O.; Kageyama, H.; Ishikawa, H.; Miyoshi, T.; Matsuoka, M. (1999): Determination of ionic self-diffusion co-

efficients of lithium electrolytes using the pulsed field gradient NMR. *J. Power Sources*, vol. 81–82, pp. 772–776.

Soetens, J.; Millot, C.; Maigret, B. (1998): Molecular dynamics simulation of $Li^+BF_4^-$ in ethylene carbonate, propylene carbonate, and dimethyl carbonate solvents. *J. Phys. Chem.*, vol. 102, pp. 1055–1061.

Takeuchi, M.; Kameda, Y.; Umebayashi, Y.; Ogawa, S.; Sonoda, T.; Ishiguro, S.; Fujita, M.; Sano, M. (2009): Ion–ion interactions of $LiPF_6$ and $LiBF_4$ in propylene carbonate solutions. *J. Mol. Liquids*, vol. 148, pp. 99–108.

Tarascon, J.-M.; Armad, M. (2001): Issues and challenges facing rechargeable lithium batteries. *Nature*, vol. 414, pp. 359–367.

Tsunekawa, S.; Narumi, A.; Sano, M.; Hiwara, A.; Fujita, M.; Yokoyama, H. (2003): Solvation and ion association studies of $LiBF_4$–propylenecarbonate and $LiBF_4$–propylenecarbonate–trimethyl phosphate solutions. *J. Phys. Chem. B*, vol. 107, pp. 109626–109666.

Ue, M. (1994): Conductivities and ion association of quaternary ammonium tetrafluoroborates in propylene carbonate. *Electrochim. Acta*, vol. 39, pp. 2083–2087.

Vincenti, W. G.; Kruger Jr., C. H. (1965): *Introduction to Physical Gas Dynamics*. New York, Wiley.

Yasui, T.; Rahong, S.; Motoyama, K.; Yanagida, T.; Wu, Q.; Kaji, N.; Kanai, M.; Doi, K.; Nagashima, K.; Tokeshi, M.; Taniguchi, M.; Kawano, S.; Kawai, T.; Baba, Y. (2013): DNA manipulation and separation in sublithographic-scale nanowire array. *ACS Nano*, vol. 7, pp. 3029–3035.

Zhang, S. S. (2006): A review on electrolyte additives for lithium-ion batteries. *J. Power Sources*, vol. 162, pp. 1379–1394.

Zhao, J.; Wang, L.; He, X.; Wan, C.; Jiang, C. (2008): Determination of lithium-ion transference numbers in $LiPF_6$–PC solutions based on electrochemical polarization and NMR measurements. *J. Electrochem. Soc.*, vol. 155, pp. A292–A296.